Spring 2021

Application of Laser Assisted Ultrasonic Nanocrystal Surface Modification on Aluminum and 3D Printed Titanium

Eman Hassan
eh40@zips.uakron.edu

Thomas Crouse
tdc20@zips.uakron.edu

Application of Laser Assisted Ultrasonic Nanocrystal Surface Modification on Aluminum and 3D Printed Titanium

Eman Hassan, Thomas Crouse, Manigandan Kannan, Yalin Dong

The University of Akron

Contents

Abstract

A novel surface treatment, laser assisted ultrasonic nanocrystal surface modification (LA-UNSM), has proved effective in increasing surface hardness, and fatigue life. The objective of this research is to determine the effectiveness of this process on components created with additive manufacturing. To accomplish this, we investigated the effectiveness of LA-UNSM treatment on aluminum, a common 3d printed metal, and the effectiveness of LA-UNSM processing on 3d printed titanium.

We first conducted our own literature review to assess the practicality of using this same treatment on aluminum. We then treated traditionally manufactured aluminum at varying levels of laser intensity to determine if this process was valid for aluminum. The low recrystallization temperature of aluminum was noted as a concern. Proceeding with our plan we treated aluminum samples at varying levels of laser power while using the same UNSM processing parameters. Hardness tests were conducted to determine the effect of the treatment, from this data a conclusive trend was difficult to identify.

In looking into the effectiveness of this process on 3d printed material, we used a sample of 3d printed titanium provided to us by colleagues. We compared the effectiveness of LA-UNSM treatments on traditionally produced titanium to the 3d printed sample using the same processing parameters with each. These samples we compared with hardness tests and microscopic surface inspection to evaluate the roughness and hardness of the samples before and after processing. These results confirmed the effectiveness of LA-UNSM treatments on titanium materials as well as demonstrated the possibility to use this process on 3d printed surfaces.

Our exploration of the effects of LA-UNSM processing on titanium, of conventional and 3d printed manufacture, shows the LA-UNSM process works on 3d printed material as well as

on traditional manufactured surfaces. The investigation of the effects of LA-UNSM treatment on aluminum was less clear. There was an improvement of the surface hardness with treatment, but further investigation is required into the effect of the laser alone on the surface.

Introduction

Ultrasonic Nanocrystal Surface Modification, UNSM for short, is a surface treatment that involves a carbide tip impacting the material at a frequency greater than that of sound, as it moves across the surface. UNSM treatment has been shown to create nano-scale microstructure while improving surface hardness and surface roughness (Efe et. all, 2020). This treatment has been further improved by the addition of a Laser. The laser anneals the cold work done by the UNSM process allowing greater plastic deformation of the surface than UNSM alone (Liu et. All 2018). This new technique has been thus called, Laser Assisted Ultrasonic Nanocrystal Surface Modification, LA-UNSM for short, and has potential for further improvement to surface hardness and a reduced surface roughness.

UNSM and LA-UNSM on a flat plate is performed in a rectangular area. The vibrating tip moves across the surface in one direction first, upon reaching the end of the rectangular area the tip advances normal to the original direction, a distance called the interval, before traversing to the opposite side of the rectangular area where it again moves normal to the original direction. This process repeats until progressing across the designated rectangular area. This process is illustrated below in Figure 1. A note not made clear by the picture is that the sequential passes across the surface overlap as the tip is larger than the interval.

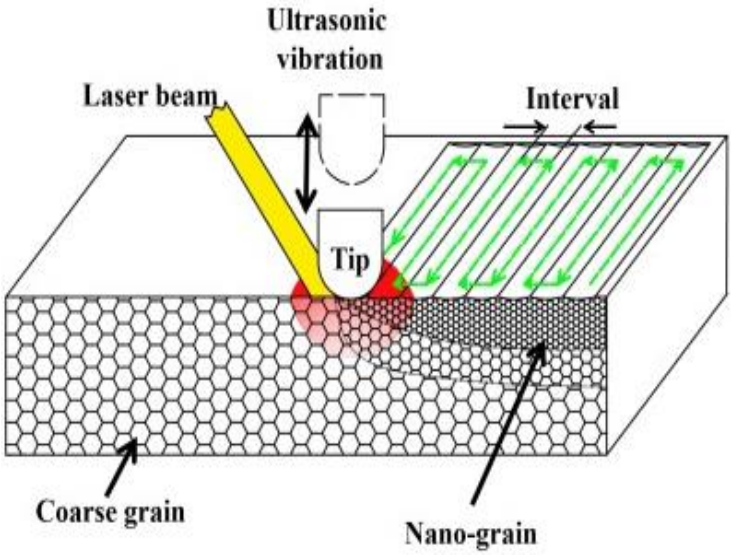

Figure 1.The LA-UNSM process, parameters, and direction. Image from "Microstructure evolution in Ti64 subjected to laser-assisted ultrasonic nanocrystal surface modification" (Liu, 2018) .

We have set out to determine if the same holds true for treatment of 3d printed materials that often have a rougher surface than traditionally manufactured materials. To accomplish this, we used identical LA-UNSM processing parameters on 3d printed titanium and conventionally produced titanium and examined the surface after treatment as well as conducted hardness tests on the surface to compare the effect. We also evaluated the effect of UNSM and the untreated material for reference.

As this process has only been tested on titanium, we wanted to see how it worked on other materials commonly used in 3d printing. We chose aluminum 7075-T6 as the material to use. With our aluminum samples we compared the untreated surface to a surface treated only with UNSM, as well as surfaces treated with LA-UNSM, at varying levels of laser power to determine where, if any, effective surface treatment could be performed on aluminum with the novel LA-UNSM treatment. We then compared the hardness of the aluminum after surface treatments.

Process

Research

From our literature review we found no information pertaining to LA-UNSM on aluminum materials. Searching for LA-UNSM in general, we found only the research that inspired this experiment, pertaining to LA-UNSM on titanium (Liu et al, 2018).

There is documentation of UNSM processes being used with success on aluminum. UNSM induces severe plastic deformation (SPD) into the processing material. The process alters the surface layer and thereby increases the performance of the material by, reducing grain size, creating residual stresses, creating dislocations in the crystal structure, and smoothing of the surface. This process also leaves the inner section of the material unaltered, allowing the retention of the materials ductility. These changes correlate to improved fatigue resistance, and hardness. (Efe et al, 2020)

The SPD process used in UNSM is a surface treatment. Furthermore, only a small depth of the material experiences this deformation. Inducing a large plastic strain into a material will effectively change its microstructure by creating ultra-fine grain (UFG). Figure 1 shows how grain size can be reduced at the surface of the material. As a result of SPD, dislocations are introduced into the material. The ability to continue plastic deformation is a function of how much dislocations can move within the microstructure. By using SPD to create UFG, the new, small grain boundaries hinder dislocation movement and hardness is increased (Mohan et al, 2016).

Some equations found which express the stress-strain behavior based on strain rate or temperature are the Zener-Holloman equation and the flow stress equation.

$$Z = \dot{\varepsilon} \exp\left(\frac{Q}{RT}\right)$$

$$Y_f = f(\varepsilon, \dot{\varepsilon}, T)$$

where $\dot{\varepsilon}$ is the strain rate, ε is the strain, Q is activation energy, R is the universal gas constant, and T is the temperature.

We consulted equilibrium phase diagrams to consider what kind of precipitates we might expect in our material as it is heated by the laser. Since it is significantly easier to find binary phase diagrams, we looked for diagrams relating aluminum to the alloying components with a significant weight contribution (>1%). These are Zinc (Zn: 5.6wt% & 2.4 at%) Magnesium (Mg: 2.5wt% & 2.8at%) Copper (Cu: 1.6wt% & 0.7at%), shown in the following Figure 2(ASM International).

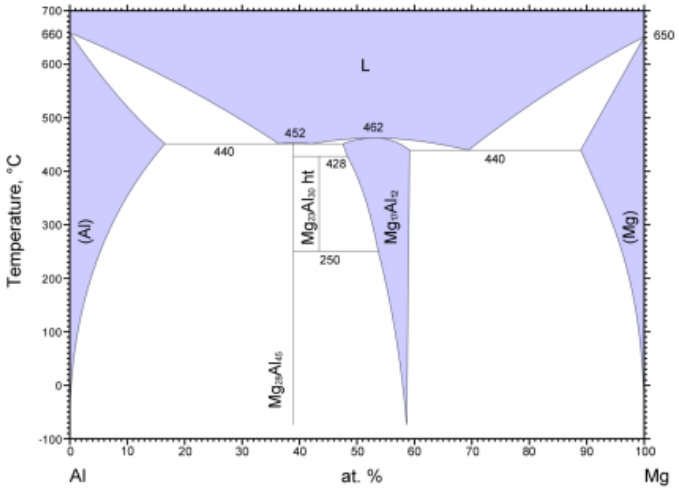

a.

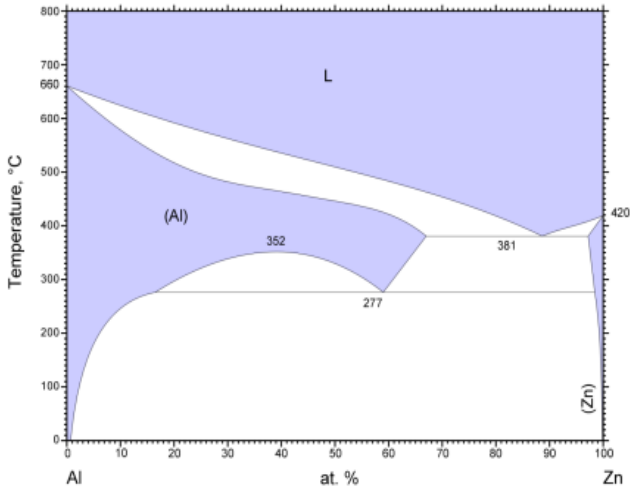

b.

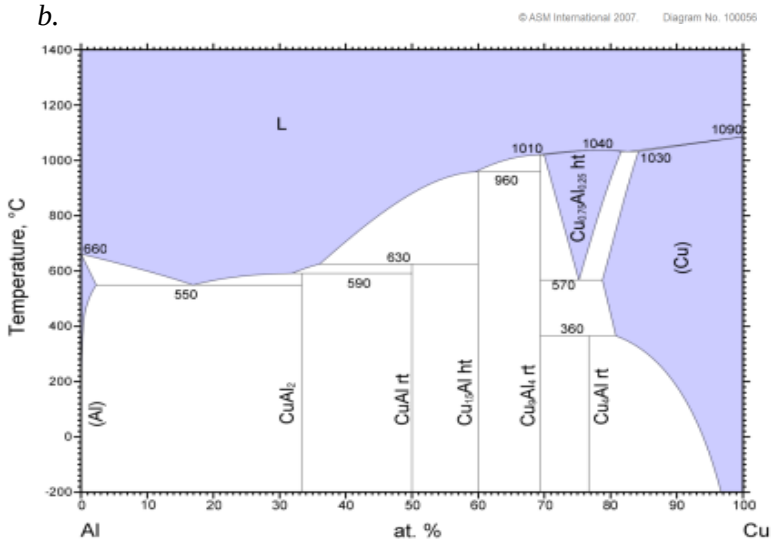

c.

Figure 2. a) Al-Zn eutectic phase diagram, b) Al-Mg eutectic phase diagram, and c)Al-Cu. eutectic phase diagram (Figures copyright ASM International 2006-2008).

For the respective weight compositions of each alloying agent as the aluminum alloy is heated (upwards of 100° C) the alloying elements separate from the alloy. This may allow the Zn and Mg to interact with one another forming the $MgZn_2$ precipitate that is desired for hardening and the objective of the artificial aging process the aluminum underwent prior to our receiving of the sample from the manufacturer. Artificial aging is often done at temperatures upwards of 150°

C to ensure the alloying elements separate from the aluminum to form the larger and stronger $MgZn_2$ precipitate.

An additional concern or consideration was the recrystallization temperature of the aluminum. For pure aluminum, the recrystallization temperature is 80°C (significantly below the melting temperature of 660°C). The recrystallization temperature is the temperature at which the dislocations in the crystal structure, that are responsible for the increase in the yield strength of the material, are repaired (Callister & Rethwisch, 2010). To alleviate this issue, we intend to keep the laser power low enough so that the deformations caused by the UNSM process are not completely removed as they are created by the laser.

Due to the low recrystallization temperature and the comparatively high temperature for precipitate to form, hardening from the forming of precipitate is unlikely at temperatures where we expect the laser to be most effective.

An important consideration for this experiment is whether the addition of laser will reverse the desirable effects of UNSM. Retrogression and Re-Aging (RRA) is a process used for reducing stress corrosion cracking in aluminum alloys while retaining strength. The RRA process could clarify the effects of the laser on aluminum. The first step of RRA is retrogression which includes short duration heat treatment at high temperatures. Retrogression is thought to dissolve microstructural precipitates within aluminum which reduces its strength (Herring, 2020). Furthermore, the temperatures associated with retrogression are 180 to 280° C. The aluminum is heated at these temperatures for 5-2400 s (Ozer, 2017). There might be a parallel between retrogression and LA-UNSM which could lead to an optimum laser temperature and processing time.

Treatment

The surface treatment was carried out by combination of a UNSM machine and a separate laser. The UNSM machine was controlled by the following parameters: scanning speed, amplitude, interval, static load, and tip size. The laser's power was another variable controlled in the treatment. The UNSM parameters for each material were held constant throughout the experiment and are listed below in Table 1.

Table 1

UNSM Parameters	Aluminum	Titanium
Scanning speed (mm/min)	500	1000
Amplitude (%)	10	30
Interval (mm)	0.07	0.01
Static Load (kg)	1	5
Tip Size (mm)	4	2.4

While processing the aluminum, the laser power was the experimental variable while others were held constant. Our intention was to determine the optimal laser power (if any) for LA-UNSM treatment. The laser power was increased by 10W increments from a minimum of 20W to a maximum value of 60W. By that point, the samples began to spark frequently during treatment, and we did not feel safe increasing the power further.

For the titanium experiments, the experimental variable was the method of production as such the laser power was kept constant across both titanium samples at 56W. This value was determined by prior research into the ideal laser power for LA-UNSM treatment on titanium (Liu et al, 2018).

Hardness Test

One purpose of this treatment is to increase the surface hardness of the material. To test the results of the treatment, we conducted several standard hardness tests on our processed samples, namely Rockwell hardness and Vickers microhardness tests. The Rockwell and Vickers tests are outlined in ASTM standards E18 and E92 respectively.

We began using Rockwell tests in different scales. For aluminum Rockwell A, C, and 30N were used; and for titanium, Rockwell 15N. These N scales being superficial Rockwell tests. These different scales use different loads, but the same basic three step procedure is utilized. The 120° diamond conical indenter is pressed into the surface with a minor load force (A). After which the major load is added (B), pressing the indenter further into the surface. After a dwell time, the major load is removed so the minor load is the only remaining force (C). After the application of the major load the preload force holds the indenter deeper in the material than it did initially due to plastic deformation. This change of depth is used to derive the Rockwell hardness through the following equation (ASTM E18, 2018).

$$HR = E - \frac{depth\ change\ (mm)}{s}$$

Below, Figure 3 illustrates the various steps in the Rockwell hardness test from left to right. Table 2 lists the different loads involved in each scale as well as variables used in the above calculation.

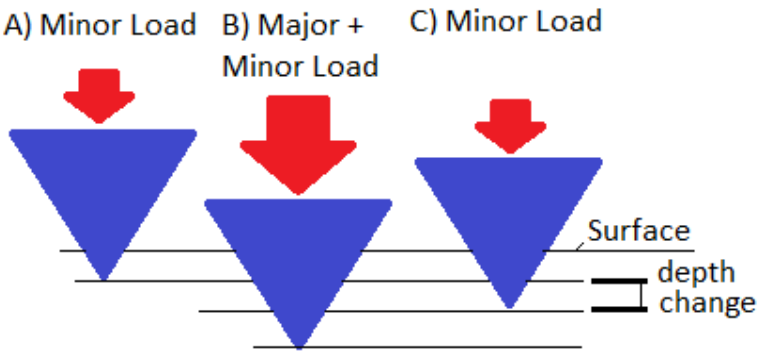

Figure 3.Shows the progression of loading in a Rockwell hardness test and the measured change of depth as described above.

Table 2

	Preload (kgf)	Major Load (kgf)	Total Load (kgf)	E	s (mm)
Rockwell 15N	3	12	15	100	0.001
Rockwell 30N	3	27	30	100	0.001
Rockwell A	10	50	60	100	0.002
Rockwell C	10	140	150	100	0.002

The Vickers 500g microhardness test was also used and is conducted in a slightly different manner. Like the Rockwell test, a load is applied to the indenter tip while it is held to the surface for a set amount of time, after which the indenter is removed. In this test a smaller load of 500g is used (~5N) thereby creating a smaller indent. Said indenter is shaped like a right pyramid with 136° between opposite faces at the tip.

After the indent has been made, measurements are taken of the diagonal distance across the indent with a microscope (in mm), as depicted in Figure 4 below. These diagonal measurements are averaged and from this value a hardness value is calculated by the following equation (ASTM E92, 2017).

$$HV = \frac{2F\sin\frac{136°}{2}}{d^2} \quad where\ d = \frac{d1 + d2}{2}\ and\ F = load\ in\ kgf$$

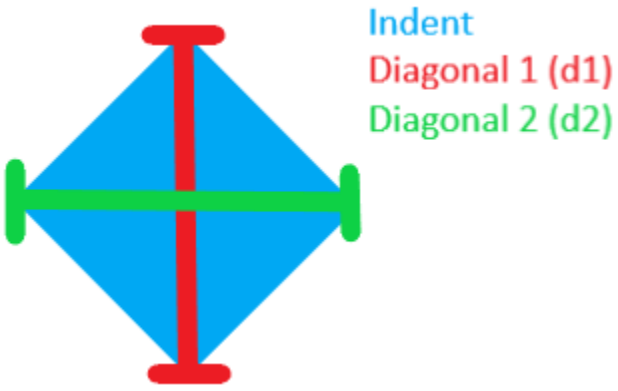

Figure 4. Shows the measured diagonal lengths, depicted in red and green, of the indent, depicted in blue.

Contact mechanics

As static hardness tests, the Rockwell and Vickers hardness are expressed through the mean contact pressure, p_m, in the material, below the indenter. This pressure can reach a value where it no longer increases with increasing force. The contact pressure is proportional to the material yield strength:

$$H = p_m \approx C \cdot Y$$

where C is a constant dependent "on the material, type of indenter, and other test conditions" (Herrmann, 2011). For a sphere indenter and completely elastic behavior, the Hertz contact relation is used:

$$a^3 = \frac{3}{4}\frac{FR}{E_r} \quad (1)$$

where *a* is the contact radius, *F* is the test force, and *R* is the radius of the indenter. To describe the interaction between the test sample and the indenter, a reduced modulus, E_r.

$$\frac{1}{E_r} = \frac{1 - v_s^2}{E_s} + \frac{1 - v_i^2}{E_i}$$

Solving for *F* in Equation 1 gives

$$F = \frac{4E_r a^3}{3R}$$

Then, substituting into

$$p_m = \frac{F}{\pi a^2}$$

gives a stress-strain relation for the mean contact pressure,

$$p_m = \frac{4E_r}{3\pi}\frac{a}{R}$$

where *a/R* is the strain penetration (Herrmann, 2011). This relation assumes a spherical indenter which the Rockwell test does not use. The Rockwell test uses a 120° cone. To get an equivalent radius we equated the surface area of the curved face of a cone to the surface area of a hemisphere. We know the indenter has a radius of 0.2mm, using the known geometry we can describe the cone height in terms of the cone radius.

$$2\pi {r_e}^2 = \pi r_c \sqrt{h^2 + {r_c}^2} = \pi r_c \sqrt{(\frac{r_c}{\tan{(60°)}})^2 + {r_c}^2}$$

Rearranging the remaining equation to solve for the equivalent hemispherical radius we arrive at.

$$r_e = 0.888 r_c = 0.178\text{mm}$$

The Hertzian contact theory can also be modified to analyze contact between a conical indenter and an elastic solid. For a conical indenter, the load relation is as follows (Fischer-Cripps, 2002).

$$F = \frac{\pi}{2} \frac{a^2 E_r}{\tan \alpha}$$

The load-point displacement of the conical indenter is given by the following equation.

$$d = \frac{\pi a}{2 \tan \alpha}$$

Solving for *a* in the two previous equations and substituting gives a relation between the load and the depth (Fischer-Cripps, 2002).

$$d = \sqrt{\frac{\pi F}{2 E_r \tan \alpha}}$$

Surface Inspection

Concerns were raised during testing as to whether the roughness of the surface could be affecting the hardness test results. We also set out to see if LA-UNSM treatment could be used to improve the roughness of a surface, specifically a 3d printed surface. To accomplish both tasks, we performed inspections of the treated and untreated surfaces, first qualitatively with an optical microscope where we noticed increase of the surface roughness of the 3d printed material from the traditionally produced titanium. To quantify this difference, we used a digital microscope to create a profile of the material surface.

Results: Titanium

Surface Inspection

Using the digital microscope, we obtained average (Ra) and maximum (Rz) roughness values across each surface reported below in Table 3. These values represent the change in height from subsequent high to low points across the whole surface (Ra) and the change in height from the 5 highest to the 5 lowest points across the whole surface (Rz).

Table 3

Reference		UNSM Reference		LA-UNSM Reference	
Ra	0 mm	Ra	0.01 mm	Ra	0 mm
Rz	0 mm	Rz	0.04 mm	Rz	0.01 mm
3d Printed		UNSM 3d Printed		LA-UNSM 3d Printed	
Ra	0 mm	Ra	0.03 mm	Ra	0.01 mm
Rz	0.01 mm	Rz	0.12 mm	Rz	0.05 mm

For reference, pictures of the samples and the sections measured are listed in the appendix.

Hardness Tests

Rockwell

Below, in Table 4, are the averaged results of the Rockwell 15N Hardness and their sample variation. It should be noted that across the materials and treatments there was little change in the measured hardness.

Table 4

	Reference		3d Printed	
	AVG	Sample Dev	AVG	Sample Dev
Untreated	76.95	0.070711	77.1	1.555635
UNSM	77.75	0.070711	70.05	7.000357
LA-UNSM	78.9	0	77.85	3.606245

Vickers

When using the Vickers microhardness test, we found a distinct change in the hardness between treatments. Reported below in Table 5 are the averaged Vickers hardness values and

the sample deviation. In the following Figure 5 is a plot of the hardness values side by side for a visual representation of the change in hardness.

Table 5

	Untreated		UNSM		LAUNSM	
	Reference	3D Printed	Reference	3D Printed	Reference	3D Printed
Average	323.6	382.7	379.6	433.8	410.3	525.4
Sample Deviation	19.9	24.7	14.3	28.9	28.7	55.4

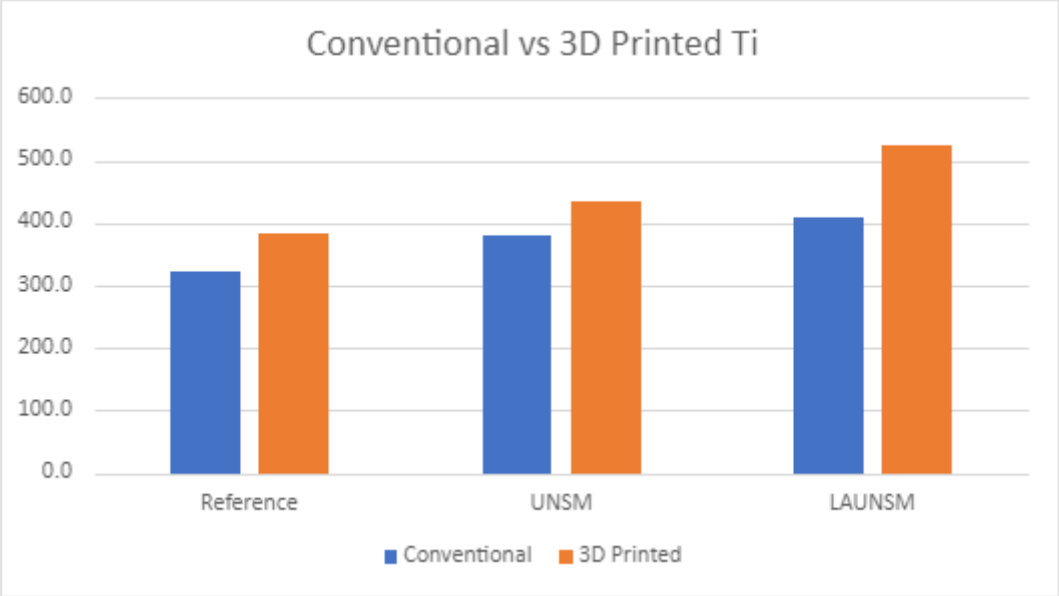

Figure 5.Side by side comparison of the Vickers hardness measurements for both types of titanium samples

Results: Aluminum

Hardness Tests

Rockwell

The averaged results of each of the three Rockwell hardness tests scales are reported in Table 6. Again, it is worth noting the lack of difference in the results for each scale.

Table 6

HRA	Untreated	UNSM	LA-UNSM				
			10%	15%	20%	25%	30%
Average	55.43333	55.43333	56.23333	56.03333	55.98333	56.01667	56.26667
Sample Dev	0.351188	1.167619	0.242212	0.463321	0.56006	0.426224	0.436654

HRC	Untreated	UNSM	LA-UNSM				
			10%	15%	20%	25%	30%
Average	10.96667	12.66667	11.43333	10.3	6.9	12.3	12.26667
Sample Dev	0.152753	0.152753	1.342882	3.464102	2.066398	0.608276	0.305505

HR30N	Untreated	UNSM	LA-UNSM				
			10%	15%	20%	25%	30%
Average	30.11667	33.73333	34.33333	34.71667	33.08333	34.43333	33.95
Sample Dev	0.617792	1.250067	0.688961	0.285774	1.083359	0.943751	1.212848

Vickers

Re-evaluating the aluminum hardness with the Vickers test produced to results displayed in the following Figure 6, showing average Vickers hardness values and the sample deviation, and Table 7 representing the same averages graphically.

Table 7

	Untreated	UNSM	LA-UNSM				
			10%	15%	20%	25%	30%
Average	176.7	200.9	140.6	188.8	192.3	247.0	247.1
Sample Dev.	12.1	49.4	26.3	46.9	47.5	35.9	31.2

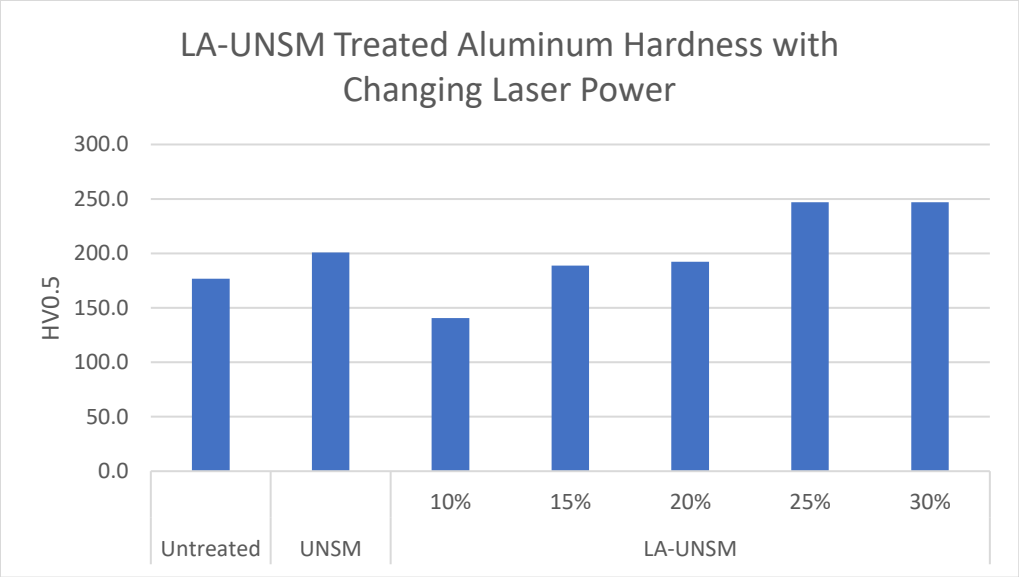

Figure 6. Shows the averaged Vickers hardness values for each treatment of aluminum samples

Discussion

The results obtained from the Rockwell tests were inconclusive showing no change between treatments. We expected to see a change between the individual surface treatments, especially the UNSM treatment as there is much documentation of this treatment being effective in increasing the hardness of a surface. We believed there to be two possible reasons for this discrepancy; the surface was too rough to provide accurate results or the Rockwell test load was too large and subsequently was penetrating too deeply, pushing through our treated region and providing inaccurate results.

To determine if the surface roughness was the source of our unexpected results, we performed the surface inspection as detailed and reported previously. These results showed an average variation of about 10 micrometers on each surface (Ra), there were some larger extreme values (Rz) on the 3d printed material on the order of 100 micrometers but upon closer inspection of the sample profile, (see appendix) there is an incline across the entire surface while in any local area the surface is rather smooth as the Ra values indicate. Furthermore, the 3d printed sample we were provided with had marks from a clamp of some kind that was applied to it prior (we were unable to find the exact origin of these marks). In the treated area of the surface, these dimples were smoothed significantly, as can be seen in the following photos labeled Figure 7. The deviation in our reported Rockwell results also suggested that the results did not fluctuate much. The highest sample deviation value, the 3d printed UNSM sample, was only 10% of the average hardness value.

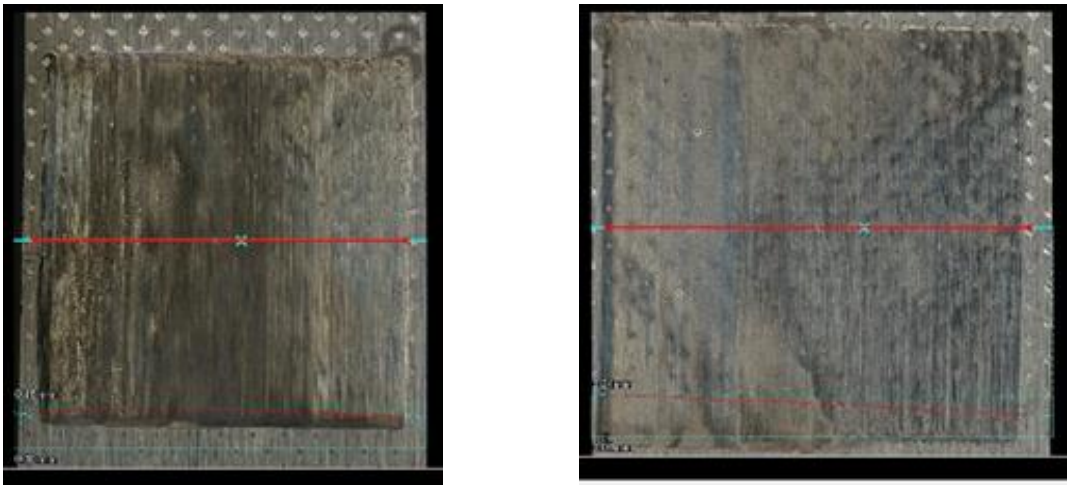

Figure 7. Left 3d printed sample processed with LA-UNSM. Right 3d printed sample with UNSM treatment. The presence of dimples on both should be noted.

Regarding the improvement of the surface roughness of 3d printed surfaces through UNSM treatment, it is difficult to declare it as a success or a failure. The sample we received, as mentioned already, was pockmarked with small blemishes from some type of clamping on a large portion of the surface. This pitted area overlapped both the UNSM and LA-UNSM test areas. The profiling data shows an increase in roughness with these two treatments, but it does not consider the preexisting roughness. It could be argued that the surface has been smoothed by these treatments but further investigation on an unblemished sample would be worthwhile.

Investigating the depth of penetration, we used two approaches, the first involved using the hardness tests results. Rearranging the Rockwell calculation to solve for the depth change,

$$depth\ change\ (mm) = (E - HR) * s$$

and substituting the equation's constants for each scale the permanent change in depth can be calculated. It should be noted that this does not take account for the maximum penetration of the indenter when both the major and minor load are applied, nor does it include the initial penetration of the indenter under the minor load. Only the change between steps A and C as described previously. The average and maximum change of indenter depths for each scale are

reported in Table 8. These values exceed our expected SPD layer thickness of 10-20μm (Liu et al, 2018).

Table 8

Aluminum						Titanium	
Rockwell 30N		Rockwell A		Rockwell C		Rockwell 15N	
Max	Average	Max	Average	Max	Average	Max	Average
70.6μm	66.5μm	93.0μm	88.7μm	191μm	178μm	30.0μm	23.6μm

To quantitatively analyze the Rockwell hardness results, theoretical calculations of the indenter penetration depths were found using the Hertzian contact theory (Table 10). These theoretical depths were then compared with the actual penetration depths in Table 8. The Rockwell tests were performed on two different materials. As such, these calculations needed to be done for both aluminum and titanium. Table 9 shows the material constants used for calculation (Callister & Rethwisch, 2012), as well as the calculated reduced modulus of elasticity for each material.

Table 9

Diamond Indenter		Aluminum		Titanium		Aluminum	Titanium	
E_i (GPa)	ν_i	E_s (GPa)	ν_s	E_s (GPa)	ν_s	E_r (GPa)	E_r (GPa)	R (mm) equiv.
1140	0.07	71.7	0.33	103	0.34	75.2	106	0.178

With the above values, the theoretical depth can be calculated as follows in Figure 15.

Table 10

	HR30N (Al)	HRA (Al)	HRC (Al)	HR15N (Ti)
Force, *F* (N)	294	588	1470	147
Change in depth, *d* (μm)	59.6	84.2	133.2	35.5

The theoretical penetration depths for Aluminum were all lower than the actual calculated depths. However, the values for the 30N and A scale were close in range to the average actual

depths. On the other hand, the theoretical depth for Titanium was higher than the actual depth but was close in range.

After determining the Rockwell test was likely penetrating the treated surface layer, we moved to a Vickers hardness test and reevaluated the hardness of the samples, both titanium and aluminum. The titanium results showed the expected increase in surface hardness from the untreated to the UNSM treatment and again from the UNSM to the LA-UNSM treatment, furthermore the 3d printed titanium had an even larger increase in hardness with the LA-UNSM treatment than the conventional titanium, as shown in Table 11. This suggests the addition of the laser is particularly effective on the 3d printed surface.

Table 11

	Untreated	UNSM	LAUNSM	UNSM – Untreated =	LA-UNSM – Untreated =	LA-UNSM – UNSM =
Conventional	323.6	379.6	410.3	56.0	86.7	30.7
3D Printed	382.7	433.8	525.4	51.1	142.7	91.5
3D – Conventional =	59.1	54.3	115.0	-4.9	55.9	60.8

The results from the aluminum are interesting. There is less of a clear-cut pattern in the results when the sample deviation is considered as shown by the box and whisker plot labeled as Figure 8. The results suggest the addition of the laser initially lowers the hardness of the material, but with increasing laser power we increase the hardness of the material. One possible explanation for this could be that the temperature of the aluminum has increased to a high enough point to cause precipitates to form readily in the material while the UNSM process is taking place at a rate that the expected annealing is offset. Further investigation with measurement of the sample's temperature during processing, and examination of precipitates present in samples from the different laser operating points, would be required to confirm this.

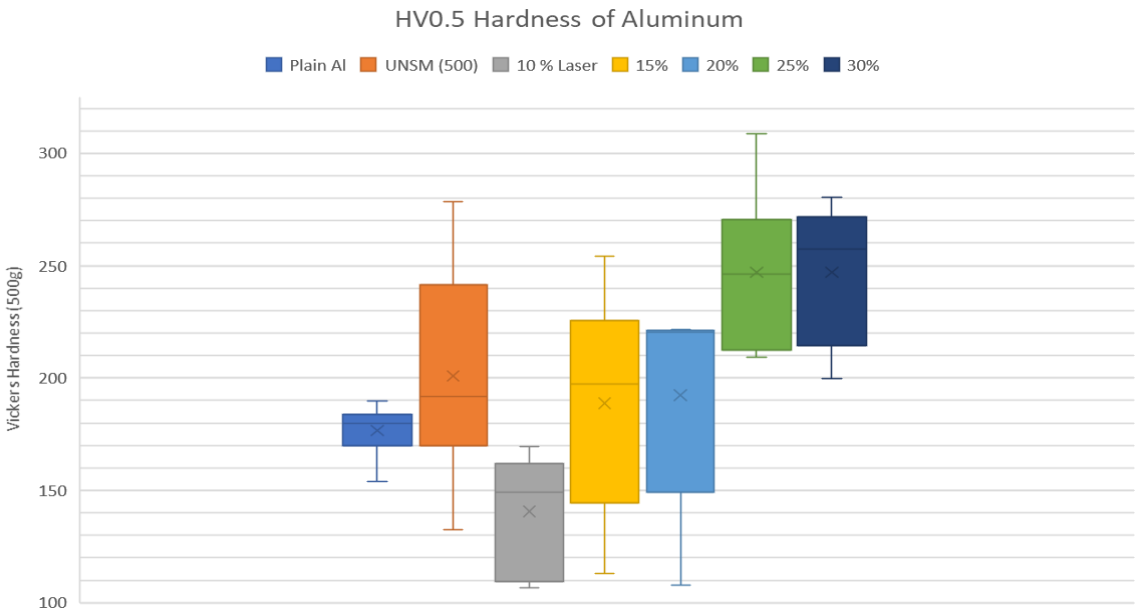

Figure 8. Plot of full Vickers hardness test results for aluminum to demonstrate variations.

Conclusion

The data supports that LA-UNSM treatment works on 3d printed material equally as well as conventionally produced material. In our data, there was a greater hardness increase in the 3d printed material. Although the 3d printed control titanium hardness was higher than the conventional control, the difference between the two doubled with the LA-UNSM treatment.

With regard to the reduction in surface roughness of 3d printed material, the data shows an increase in the surface roughness with both UNSM and LA-UNSM treatment. We believe this may be incorrect and that preexisting surface roughness in the areas of surface treatment have skewed the results. We suggest further investigation into this field with undamaged samples.

LA-UNSM treatment of aluminum shows an increase in surface hardness over plain UNSM at laser power levels greater than 50W. This may not be due to the LA-UNSM treatment and instead due to the laser alone. Further investigation into the effect of the laser, and the subsequent composition and microstructure of the material is strongly recommended to determine if this hardness increase is due to the LA-UNSM treatment or another source.

References

ASM International. (n.d.). Alloy Phase Diagram Database. Retrieved April 01, 2021, from https://matdata.asminternational.org/apd/index.aspx

ASTM Standard E18, 2018, "Standard Test Methods for Rockwell Hardness of Metallic Materials" ASTM International, West Conshohocken, PA, DOI: July 1, 2018, www.astm.org

ASTM Standard E92, 2017, "Standard Test Methods for Vickers Hardness and Knoop Hardness of Metallic Materials" ASTM International, West Conshohocken, PA, DOI: April 1, 2017, www.astm.org

Callister, W. D. (2001). Fundamentals of materials science and engineering: An interactive. New York, NY: John Wiley & Sons.

Callister, W. D., & Rethwisch, D. G. (2012). *Materials science and engineering: An introduction*. Hoboken, NJ: John Wiley & Sons.

Chinella, J., & Guo, Z. *Computational Thermodynamics Characterization of 7075 ...* https://apps.dtic.mil/dtic/tr/fulltext/u2/a553561.pdf.

Efe, Y., Karademir, I., Husem, F., Maleki, E., Karimbaev, R., Amanov, A., & Unal, O. (2020). Enhancement in microstructural and mechanical performance of AA7075 aluminum alloy via severe shot peening and ultrasonic nanocrystal surface modification. *Applied Surface Science*, *528*, 146922. https://doi.org/10.1016/j.apsusc.2020.146922

Fischer-Cripps, A. C. (2002). Nanoindentation. In *Nanoindentation* (pp. 101-108). New York, NY: Springer.

Herring, D. (2020, February 7). Retrogression and Re-aging for Aluminum Alloys (part 2). Retrieved December 09, 2020, from https://www.industrialheating.com/articles/95471-retrogression-and-re-aging-for-aluminum-alloys-part-2

Liu, J., Suslov, S., Ren, Z., Dong, Y., & Ye, C. (2018, September 24). *Microstructure evolution in Ti64 subjected to laser-assisted ultrasonic nanocrystal surface modification*. https://www.sciencedirect.com/science/article/pii/S0890695518302943.

Low III, S. R. (2001). NIST Recommended practice guide: Rockwell hardness measurement of metallic materials.

Mohan, K., Suresh, J.A., Ramu, P. et al. Microstructure and Mechanical Behavior of Al 7075-T6 Subjected to Shallow Cryogenic Treatment. J. of Materi Eng and Perform 25, 2185–2194 (2016). https://doi.org/10.1007/s11665-016-2052-1

OZER, G., KARAASLAN, A., Properties of AA7075 aluminum alloy in aging and retrogression and reaging process, Transactions of Nonferrous Metals Society of China, Volume 27, Issue 11, 2017, Pages 2357-2362

Appendix

Titanium Surface Inspection Photos

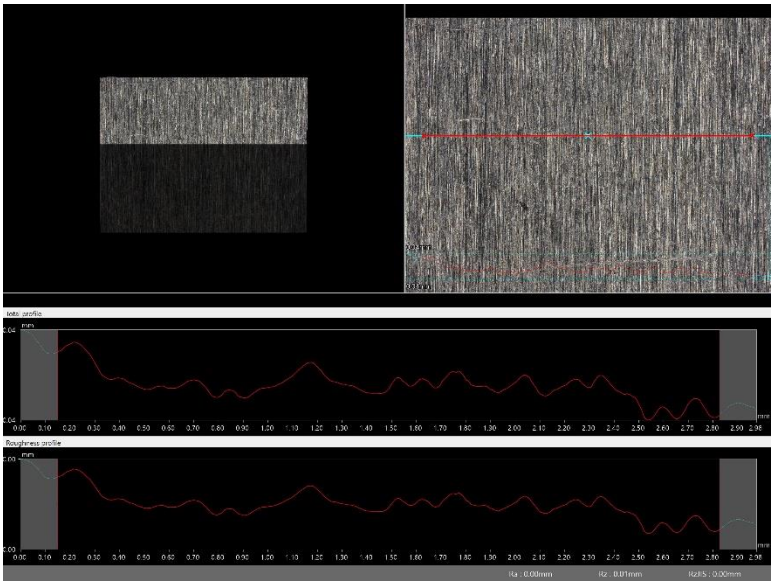

3d Titanium

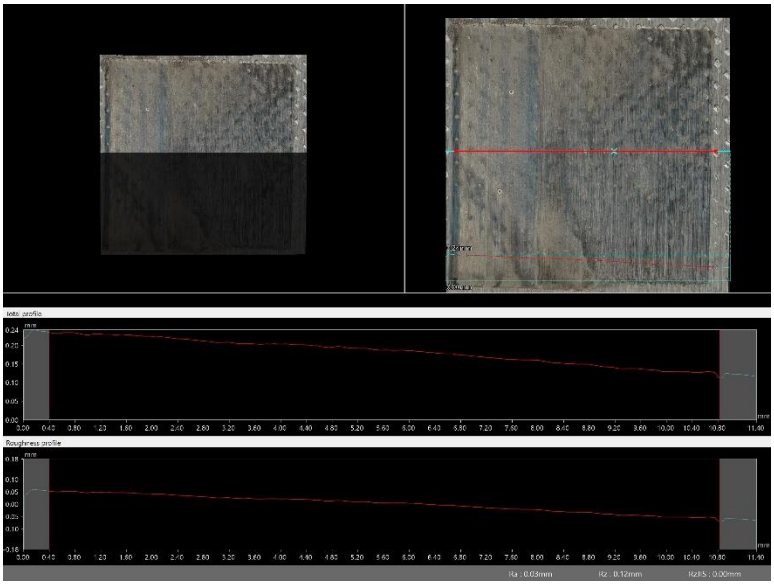

3d Titanium UNSM

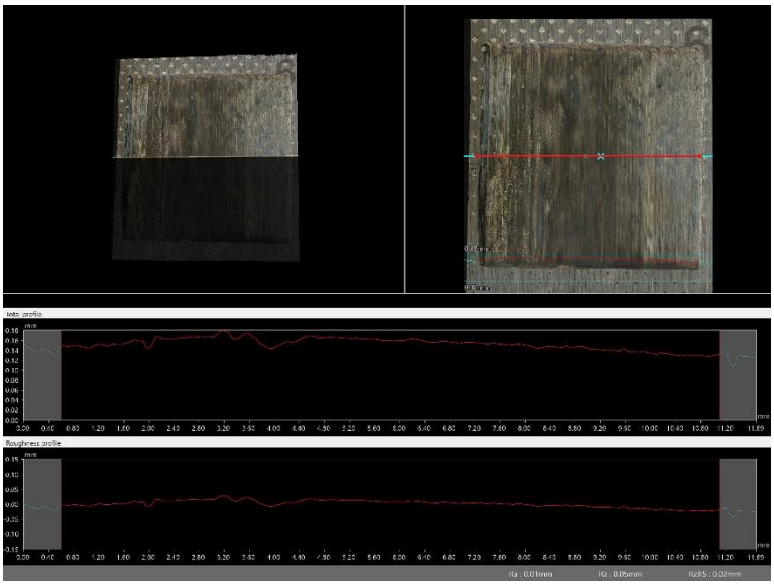

3d Titanium LA-UNSM

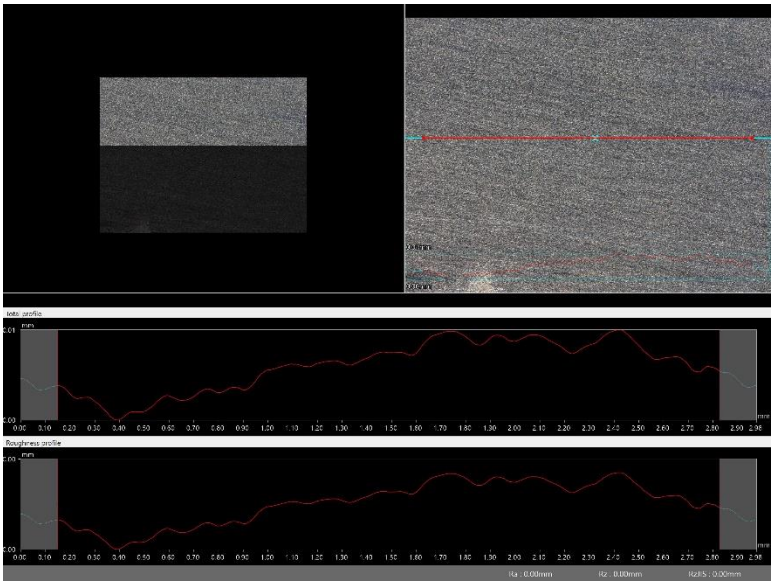

Reference Titanium

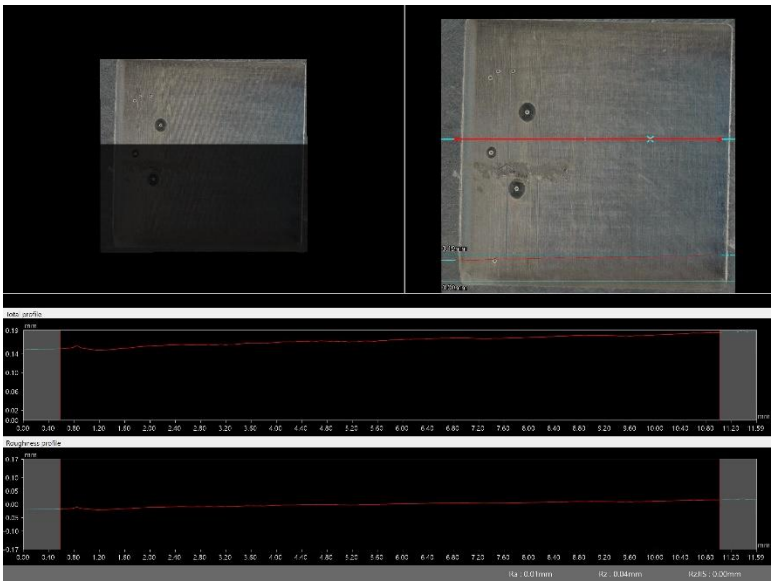

Reference Titanium UNSM

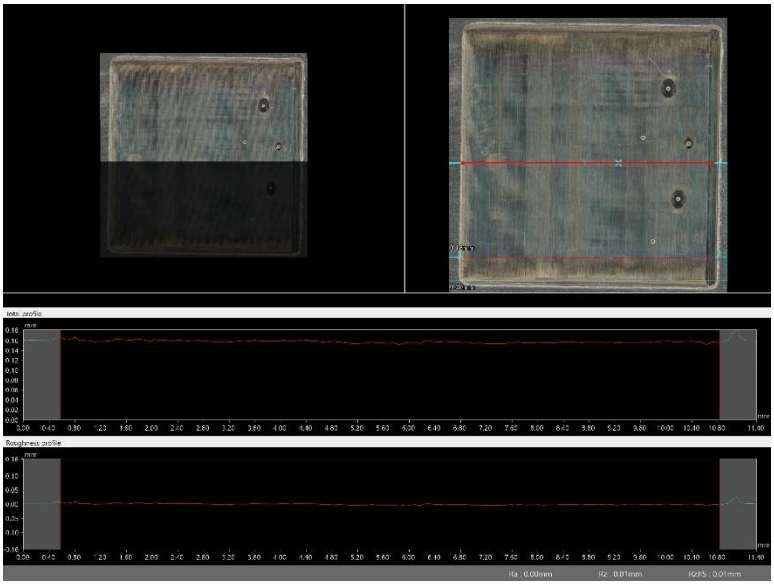

Reference Titanium LA-UNSM